# Kinetic phase-space vortices in magnetized space plasmas

**Dušan Jovanović**
Institute of Physics, P. O. Box 57
11001 Belgrade, Serbia
*djovanov@phy.bg.ac.yu*


**Padma K. Shukla**
Institute for Theoretical Physics IV, Faculty
for Physics and Astronomy, Ruhr-University Bochum
D-44780 Bochum, Germany
*ps@tp4.rub.de*

# Introduction

- Coherent nonlinear structures (electrostatic solitary waves, ESWs) ⇨ spatially localized regions with finite electric charges ⇨ ubiquitous in Earth's magnetosphere.
- Characteristic signatures ⇨ bipolar pulses of the electric field parallel to the magnetic field line documented by many satellite missions in the near-Earth plasma regions that are subject to various linear instabilities due to
- Strong particle beams
- Sharp boundaries
- Thin current sheets (also susceptible to filamentaton/ magnetic reconnection).
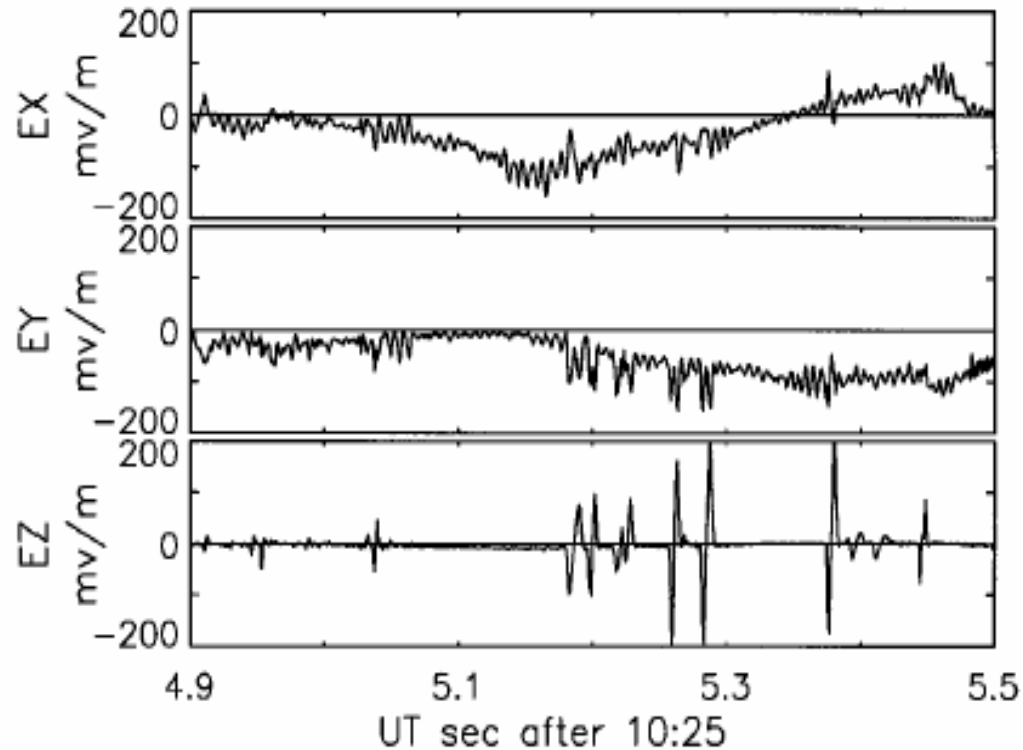
# POLAR data from the auroral region:



FIG. 1. Electric field measurements in a magnetic field aligned coordinate system in the auroral acceleration region illustrating small and large amplitude solitary waves and double layers during the 0.6 s interval after 1025:04.9 UT on 10 July 1996.

F. S. Mozer *et al.,*
Phys. Rev. Lett. **79,** 1281 (1997)
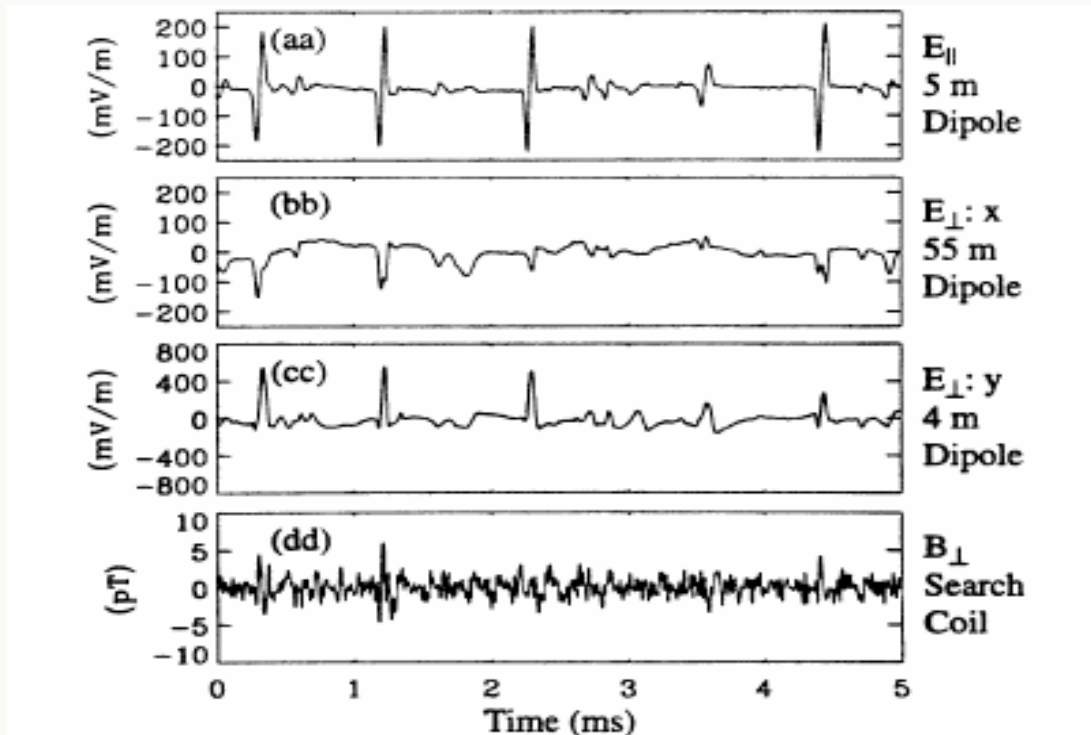
# FAST data from the auroral region :



FIG. 1.   (a) The electric field parallel to $\mathbf{B}_0$.  (b) The electric field perpendicular to $\mathbf{B}_0$ ($\Delta E_\perp$) and in the spin plane of the satellite.  This signal, measured by a 56 m dipole antenna, appears attenuated, indicating that the structure size may have been <112 m.  (c) $\Delta E_\perp$ along the spin axis of the satellite. (d) A perturbation magnetic field perpendicular to $\mathbf{B}_0$ ($\Delta B_\perp$). $\Delta B_\perp$ was filtered to a pass band (3–16 kHz) to expose the weak signals and therefore may not appear unipolar in this figure.  (aa)–(dd) An expanded view of the above data.

R. E. Ergun *et al.,*
Phys. Rev. Lett. **81,** 826  (1998)

# POLAR data from the sub-solar magnetopause:
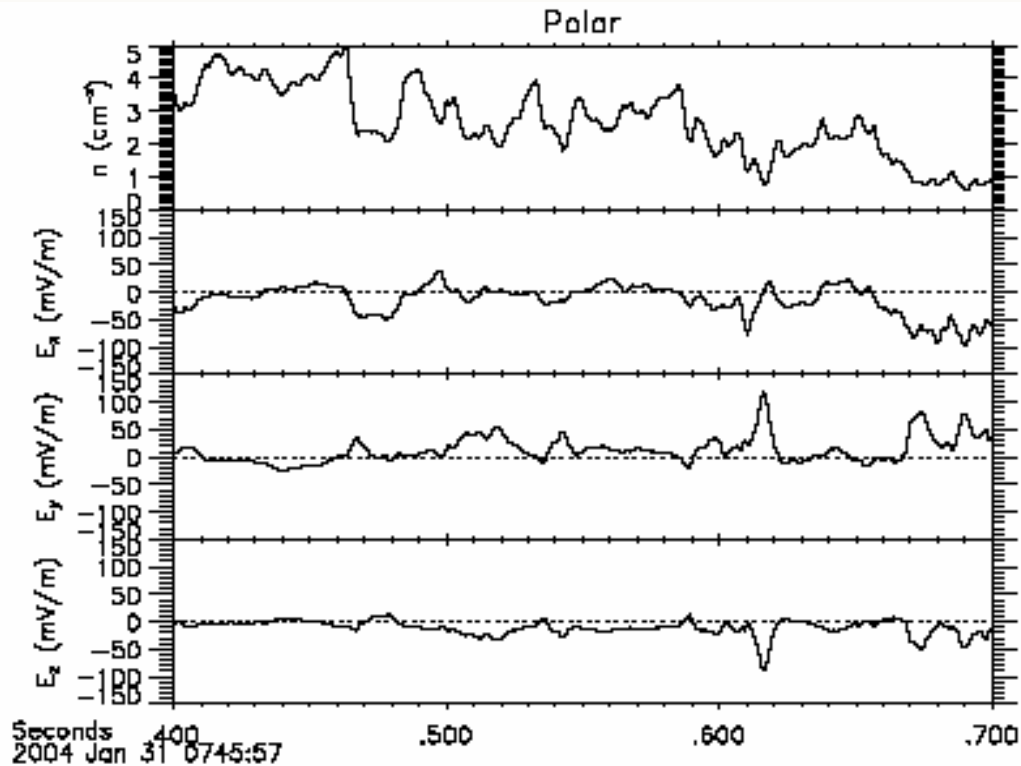


Polar

$$E_\parallel << E_\perp$$

**Figure 3.** Plasma density and the three components of the electric field measured during a 300 msec interval on the Polar spacecraft as it passed through the density decrease from the magnetosheath to the magnetosphere.

[note: Geocentric Solar Ecliptic (GSE) coordinates]

F. S. Mozer et al.
Geoohys. Res. Lett.
31, L15802 (2004)

# WIND observaton in reconnection region in magnetotail: ESWs coupled with upper-hybrid waves
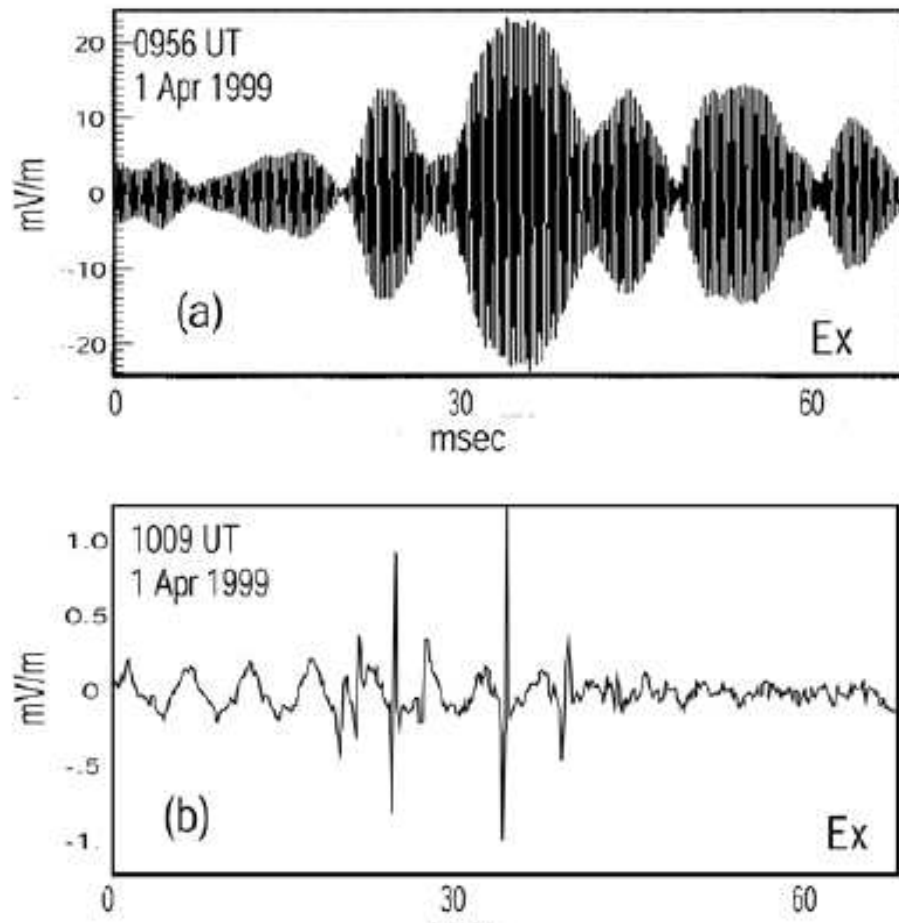


- W. M. Farrell, *et al.*, GRL 2002

**Figure 2.** Waveform from the Wind/WAVES time domain sampling system. Panel (a) displays the waveform 0956 UT on 1 April, corresponding to an intense narrowbanded emission near ~2700 Hz. This frequency is near the local upper hybrid frequency. Panel (b) shows a set of electrostatic solitary pulses responsible for the broadband electrostatic noise observed during the encounter. Panel (c) is a

- **Ponderomotive potential of the upper-hybrid wave > 10% of the ESW (slow) potential**

# WIND data - tripolar pulses in the solar wind
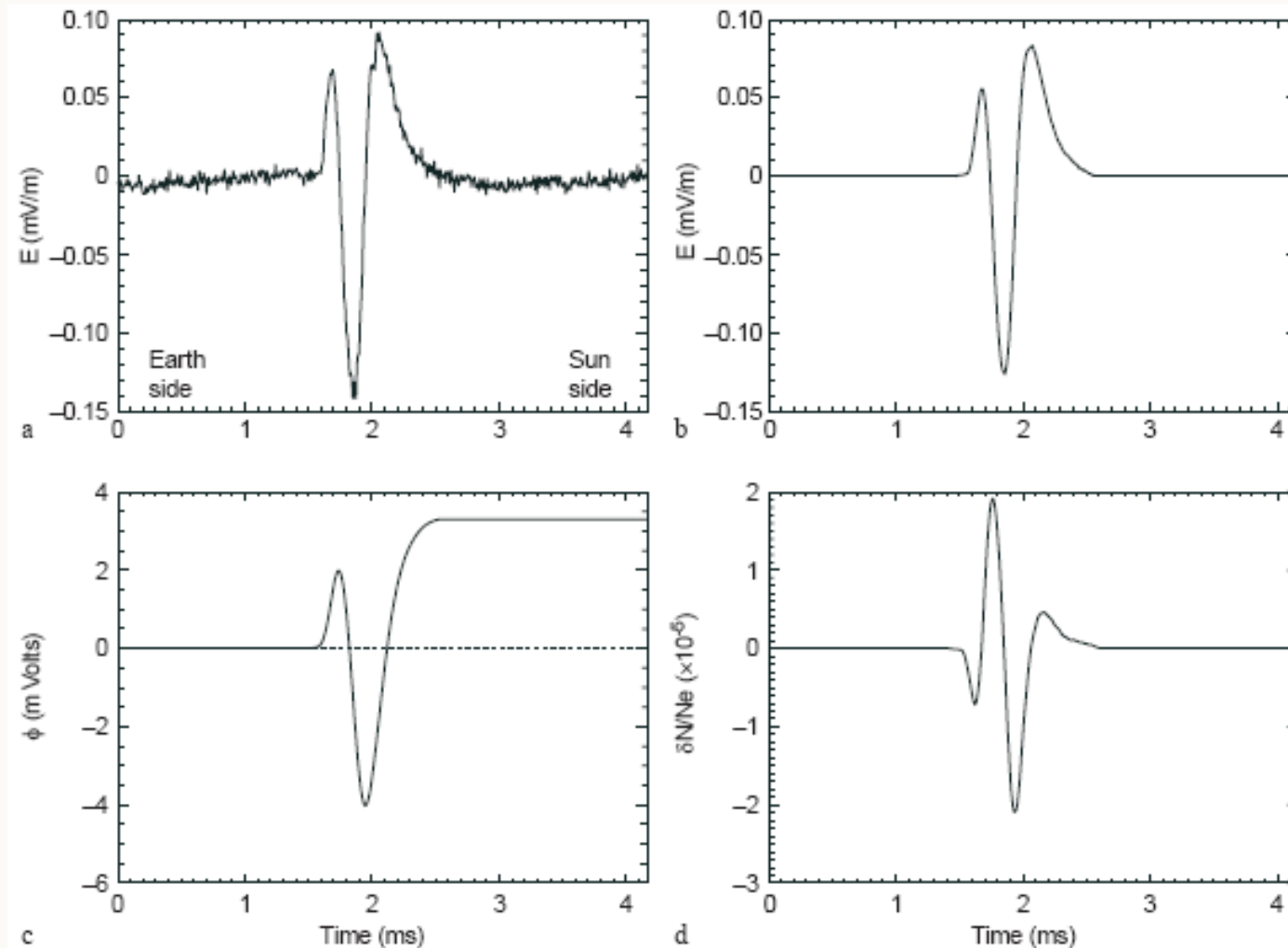


A. Mangeney *et al.*,
Ann. Geophys.
**17.** 307 (1999)

**Fig. 6a–d.** For the central double layer in Fig. 1f (between 8 and 9 ms), time profile of: a the measured electric field (positive if directed to the Earth); b the electric field smoothed over 10 points; c the corresponding potential profile; d the charge separation $\delta N = N_p - N_e$

# Properties of ESWs in the magnetosphere:

- ESWs propagate along the magnetic field lines at 250-2500 km/s, comparable to $v_{Te}$ and to the speed of the electron beams.
- The amplitude is usually less than the electron thermal energy, $e\Phi < T_e$
- The duration ranges from slightly shorter than the gyroperiod of $H^+$ ions to slightly longer than the electron plasma period.
- They appear either isolated, or in a wavetrain organized near the ion-cyclotron or lower-hybrid frequency (Ergun et al., 1998).
- Sometimes strictly one-dimensional along the magnetic field [in the deep magnetotail (Matsumoto et al., 1994; Kojima et al., 1999)].
- Often finite perpendicular size, larger than parallel size [close to bow shock (Cattell et al., 2003), in low-altitude acceleration region (Ergun et al., 1998)]
- Sometimes perpendicular size comparable, or shorter than the parallel size [in high-altitude auroral region (Mozer et al., 1997)].
- Strictly perpendicular signals in the magnetopause (Mozer et al., 2004).
- Discrepancies can not be attributed only to geometric factors (e. g. pancake structures traversed at the centre or at the edge).
- Sometimes ESWs are accompanied by large amplitude upper-hybrid waves

# Properties of ESWs in Solar wind:

- Tripolar pulses of ESWs in the Solar wind [Mangeney *et al.,* (1999), Lacombe *et al.,* (2002)].
- They feature a net potential jump – similar to double layers.
- Propagate along the magnetic field, their speed is small compared to the solar wind velocity.
- Typical spatial width is 25 $\lambda_D$.

# Earth's magnetosphere:
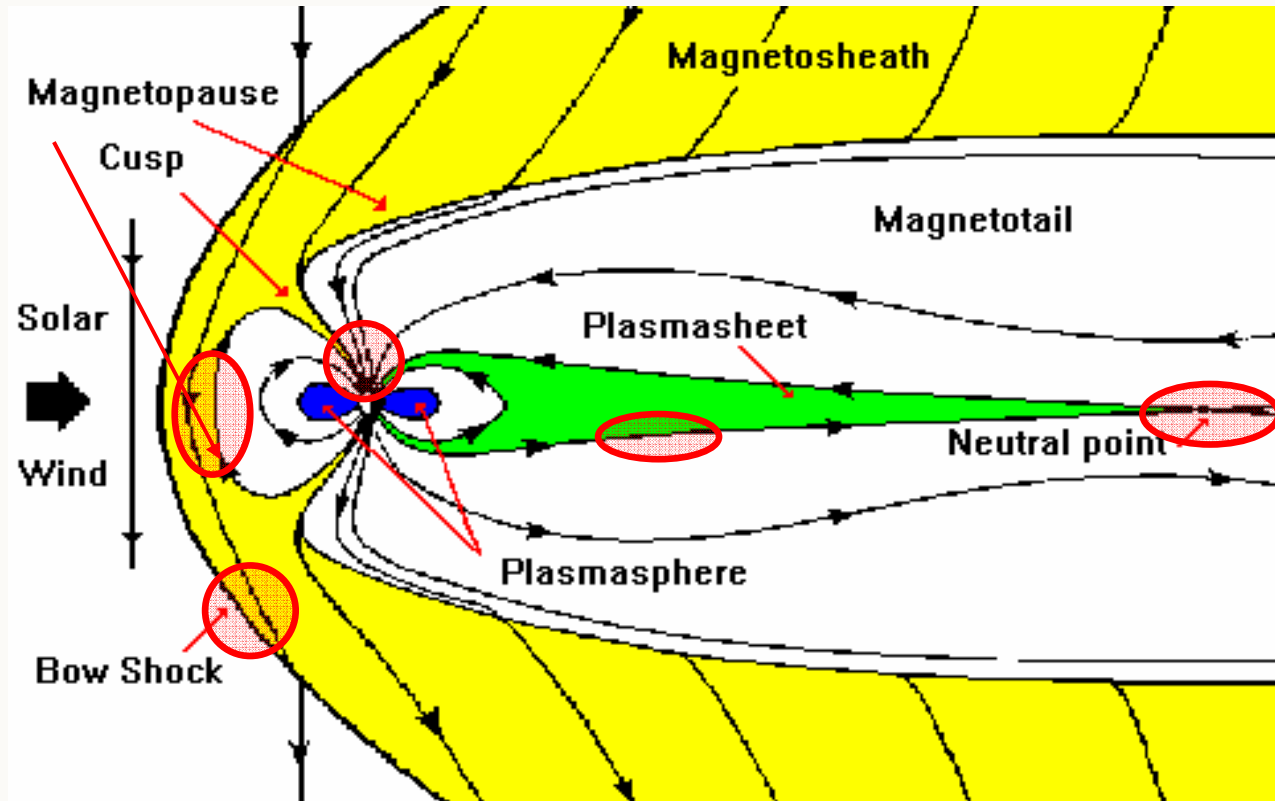


ESWs appear at sharp boundaries and within current sheets
- Magnetopause
- Magnetotail
- Auroral region
- Bow shock
- Plasmasheet boudary

# Fast reconnection ⇨ parallel electron beams ⇨ secondary instabilties

- **Strong secondary instabilities in systems with a guide field**
  - strong electron streaming near x-line and along separatrices leads to Buneman instability and evolves into nonlinear state with strong localized electric fields produced by "electron-holes"
- **In a system with anti-parallel magnetic fields (no gude magnetic field) secondary instabilities play a minor role**
  - current layer near x-line is completely stable
    - strong coupling to lower hybrid waves
  - resulting electron scattering produces strong anomalous resistivity and electron heating

# Trapping ⇨ saturation for various beam-plasma instabilities (two-stream, bump-on-tail, Buneman):



WAVE POTENTIAL

Fig. 1. Schematic illustration of particle trapping in a wave potential
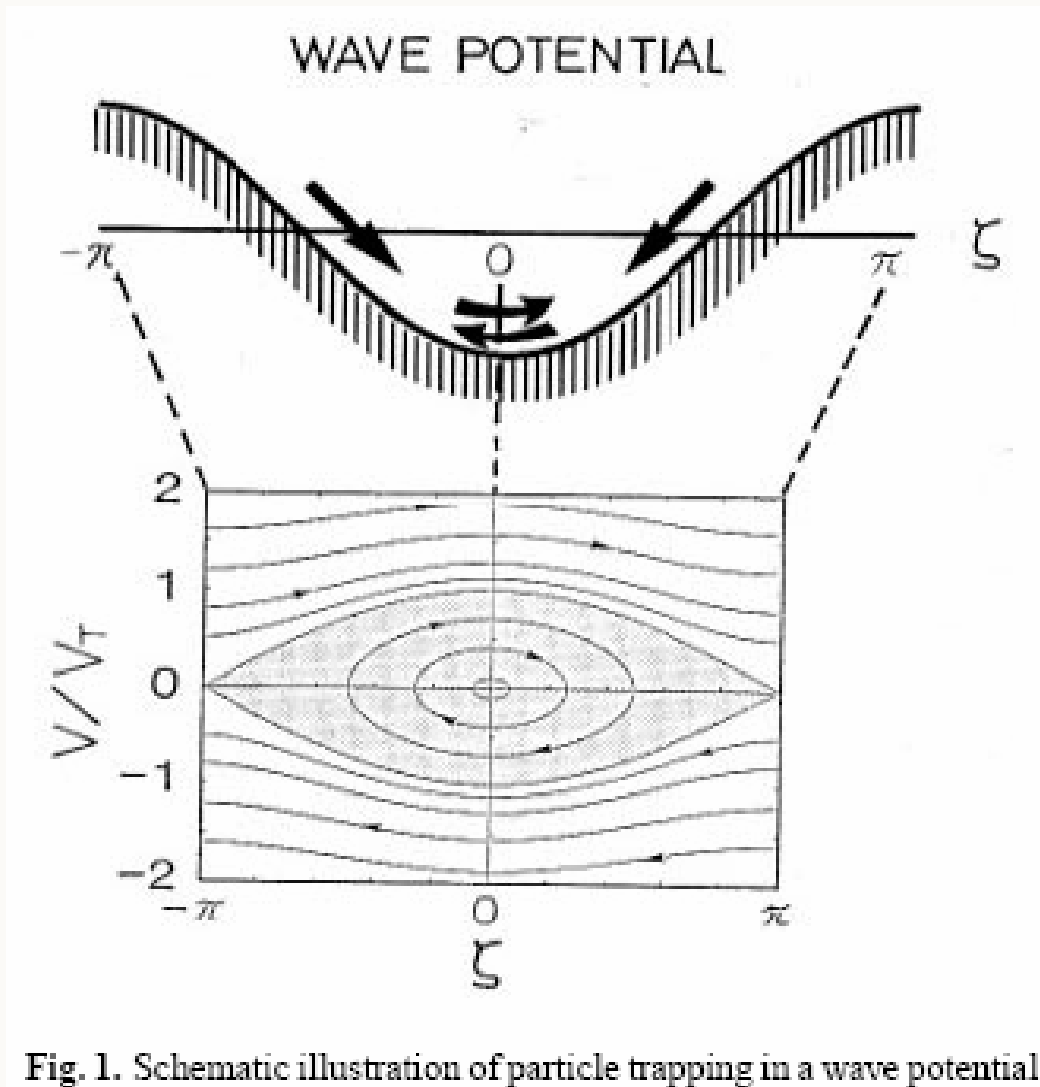
**Y. Omura, T. Umeda, and H. Matsumoto**
Proceedings of ISSS-6 (2001): 1–4 c
Copernicus Gesellschaft 2001

# Buneman instability:

$$1 + \frac{\omega_{p,e}^2}{\Omega_e^2} \frac{k_\perp^2}{k^2} - \frac{\omega_{p,e}^2}{(\omega - k_z v_{z,0})^2} \frac{k_z^2}{k^2} - \frac{\omega_{p,i}^2}{\omega^2} = 0,$$
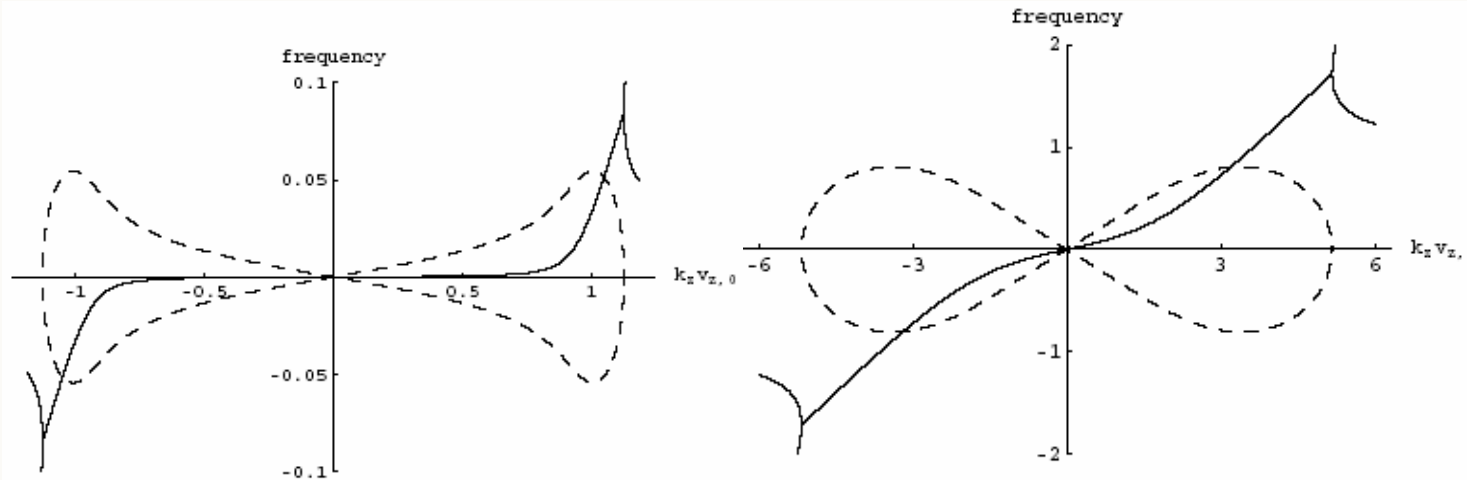


Magnetopause conditions of (Mozer et al., 2004).

**Figure 1.** Parallel propagation, $k_\perp = 0$. The real and imaginary parts of the frequency (solid and dashed lines, respectively) of a linearly unstable mode described by the dispersion relation, Eq. (8), as a function of the zero-order Doppler shift $k_z v_{z,0}$. For the parallel mode, the frequency and the Doppler-shift are normalized by the electron plasma frequency $\omega_{p,e}$. The relevant plasma parameter is adopted as $\omega_{p,e}/|\Omega_e| = \sqrt{35}$.

**Figure 2.** Oblique propagation, $\tan\theta = k_z/k_\perp = 1/15$. The real and imaginary parts of the frequency (solid and dashed lines, respectively) of a linearly unstable mode described by the dispersion relation, Eq. (8), as a function of the zero-order Doppler shift. For the oblique mode, the frequency and the Doppler-shift are normalized by the lower-hybrid frequency $\omega_{LH} = (|\Omega_e|\Omega_i)^{\frac{1}{2}}$. The relevant plasma parameter is adopted as $\omega_{p,e}/|\Omega_e| = \sqrt{35}$.

# Lower-hybrid holes:

- Standard theory considers electrons trapped by large amplitude Langmuir waves, excited by some beam-plasma instability (two-stream, Buneman, bump-on-tail).
- In a magnetized plasma the electrostatic lower-hybrid waves can be excited by the same instabilities, but with smaller growthrates.
- Strong lower-hybrid waves often observed in conjunction with ESWs in the magnetosphere.

## Lower-hybrid holes:

- Parallel-propagating Langmuir waves may saturate at a relatively low level, leaving enough beam electrons to excite lower-hybrid waves.
- Lower-hybrid waves may emerge in the decay of the Langmuir-type electron holes
- Lower-hybrid holes are much more complicated than the 1-D Langmuir holes.
- They are inherently multidimensonal and magnetized.
- One needs to determine trajectories of trapped particles in a 2-D or 3-D potential minimum, and in the presence of magnetic field.

# Nonlinear lower-hybrid waves, kinetic approach:

- Drift-kinetic description for electrons in the regime

$$d/dt << \Omega_e, \qquad e\Phi << T_e, \qquad T_{e\perp} << T_{e\parallel}, \qquad \beta = 2p/c^2\varepsilon_0 B_0^2 << 1$$

$$\left( \frac{\partial}{\partial t} + \vec{V} \cdot \nabla \right) g - \frac{e}{m_e} E_\parallel \frac{\partial g}{\partial v_\parallel} = 0,$$

$$\vec{V} = v_\parallel \vec{e}_z + (1/B_{z,0}) \vec{e}_z \times \nabla(\phi - v_\parallel A_z)$$

$$E_\parallel = -[\partial/\partial z - (1/B_{z,0})(\vec{e}_z \times \nabla A_z) \cdot \nabla]\phi - \partial A_z/\partial t.$$

$$g = \log \overline{\overline{f}}(v_\parallel) + \rho_{L,e\parallel}^2 \nabla_\perp^2 (e\phi/T_{e\parallel}),$$

$$\overline{\overline{f}} = \int dv_x \, dv_y \, f$$

# Stationary solution of drift-kinetic equation:

- Following the standard electron hole scenario (Schamel) we do not study the full plasma dynamics following the onset of the instability.
- We seek plausible stationary solutions that may be its saturated state.
- For a stationary solution moving with the velocity *uz,* using ∂/∂t = −*uz* ∂/∂z, the nonlinear characteristics of drift-kinetic equation are determined from

$$\frac{dx}{V_x} = \frac{dy}{V_y} = \frac{dz}{v_\| - u_z} = \frac{(m_e/e)\, dv_\|}{\hat{D}_\| (\phi - u_z A_z)},$$

$$\hat{D}_\| = \partial/\partial z - (1/B_{z,0})(\vec{e}_z \times \nabla A_z) \cdot \nabla$$

- In general, there are three conserved quantities

# Conservation of energy:

- The electron energy W is conserved

$$W = (m_e/2)(v_\parallel - u_z)^2 - e(\phi - u_z A_z).$$

- It is known from the nonlinear dynamics that a stable nonlinear solution can be obtained only if the number of conserved quantities matches the number of degrees of freedom of the system.

- To describe the general solution of the stationary drift-kinetic equation that is stable, we need to find all three integrals of motion.

- This is a very difficult task that requires the inversion of the unknown functions *Φ(x, y, z) and A$_z$(x, y, z).*

- The remaining integrals of motion can be expressed in a closed form only in some special cases with reduced dimensionality, when Φ and A$_z$ depend on certain prescribed combinations of spatial variables.

# Conservation of canonical momentum:

1.  Parallel solution:  We introduce orthogonal coordinates $r = r(x, y)$ and $\varphi = \varphi(x, y)$, and require that the potentials $\Phi$ and $A_z$ do not depend on $\varphi$. Then, the vector nonlinearities in $A$ and $E_\parallel$ reduce to zero, and the electron energy W is the only integral of motion.
2.  Oblique solution: We introduce new variables $y' = y + z \tan \theta$ and $z' = z - y \tan \theta$, and require that solution is independent on $z'$. This is an infinitely long homogeneous solution, tilted by the angle $\theta$. Then, there is a second integral of motion, the **canonical momentum**

$$P = m_e v_\parallel - e(A_z - x\, B_{z,0} \tan \theta).$$

# Adiabatic assumption:

- If $\Phi$ and $A_z$ were adiabatically "switched on" at $t = -\infty$ initial velocity $v^{(0)}$
- and position $x^{(0)}$ of the particle that at the moment $t$ had the velocity $v_\parallel$ and position $x$ are found for parallel solution from conserved quantities as

$$v_\parallel^{(0)} = u_z + \text{sign}(v_\parallel - u_z)[(v_\parallel - u_z)^2 - (2e/m_e)(\phi - u_z A_z)]^{1/2}$$

$$x^{(0)} = x,$$

- For oblique solution $v^{(0)}$ is the same as above, and the initial position is

$$x^{(0)} = x + (v_\parallel - v_\parallel^{(0)} - eA_z/m_e)/(\Omega_e \tan\theta)$$

- The electron distribution can now be expressed by substituting in the unperturbed distribution function the velocity $v_\parallel$ and position $x$ by their initial values $v^{(0)}$ and $x^{(0)}$, provided the evolution of the system was adiabatic throughout its history.

## Adiabatic assumption (continued):

- The initial velocity $v^{(0)}$ is complex for the particles with negative energy.
- They participated in some nonadiabatic process, since initially the energies of all particles were positive.
- They must be confined to a limited spatial region, or trapped
- We assume that the "memory" of the initial velocity of trapped particles was lost due to many oscillations inside the trapping potential.
- We adopt their distribution to be to be Gaussian, with a different temperature than the free particles (possibly negative).
- That gives the standard Schamel's distribution function, modified to account for the electron polarization.

$$\bar{\bar{f}}\left(v_{\parallel}\right) = \frac{n_0}{\sqrt{2\pi}\, v_{T,e\parallel}} \exp\left\{-\frac{1}{2v_{T,e\parallel}^2}\left[\left(\mathrm{Re}\, v_{\parallel}^{(0)}\right)^2 - \beta\left(\mathrm{Im}\, v_{\parallel}^{(0)}\right)^2\right.\right.$$

$$\left.\left. +\frac{2e}{m_e}\, \rho_{L,e\parallel}^2 \nabla_{\perp}^2 \phi\right]\right\}.$$

# Electron density and velocity:

■ The integration of the Schamel's distribution function gives:

$$n_e = n_0 \left( 1 - \rho_{L,e\parallel}^2 \nabla_\perp^2 \frac{e\phi}{T_{e\parallel}} + a\,\Phi - \frac{4}{3}\, b_n \Phi^{3/2} \right),$$

$$v_{z,e} = u_z \left( a\,\Phi - \frac{4}{3}\, b_v \Phi^{3/2} \right),$$

$$\Phi = (e/T_{e\parallel})(\phi - u_z A_z)$$

$$a = (2\pi v_{T,e\parallel}^2)^{-1/2} \int_{-\infty}^{\infty} dv_\parallel v_\parallel (v_\parallel - u_z)^{-1} \exp(-v_\parallel^2/2v_{T,e\parallel}^2)$$

$$b_n = \pi^{-1/2}(1 - \beta)\exp(-u_z^2/2v_{T,e\parallel}^2)$$

$$b_v = \pi^{-1/2}(3/2 - \beta)\exp(-u_z^2/2v_{T,e\parallel}^2)$$

# Ion response

- Cold, linear, two-dimensional ions with the zero-order velocity $v_{z,0}$ (giving rise to Buneman instability)

$$\left(\frac{\partial}{\partial t} + v_{z,0}\frac{\partial}{\partial z}\right)^2 n_i = \frac{e\,n_0}{m_i}\nabla^2\phi.$$

# Nonlinear equation for electrostatic potential

- Plug electron and ion densities, velocities into Poisson's equation and the Ampere's law
- Assume $u_z^2/c^2 \ll \min(1, a^{-1}\lambda^2_{D,e\parallel} \nabla_\perp^2)$
- Decouple these equations $\Rightarrow$ equation for NL lower-hybrid waves
- Nonlinearity comes from trapped electrons.

$$\frac{\partial^2}{\partial z^2}\left\{\lambda^2_{D,e\parallel}\left[\left(1+\frac{\omega^2_{p,e}}{\Omega^2_e}\right)\nabla_\perp^2+\frac{\partial^2}{\partial z^2}\right]\Phi-a\Phi-\frac{4}{3}b_n\Phi^{3/2}\right\}$$

$$+\frac{\omega^2_{p,i}}{(v_{z,0}-u_z)^2}\left(\nabla_\perp^2+\frac{\partial^2}{\partial z^2}\right)\Phi=0.$$

## Parallel solution (either slab, or cylindrically symmetric)

$$\frac{\partial^2}{\partial z^2}\left[\left(\nabla_\perp^2 + \frac{\partial^2}{\partial z^2}\right)\Phi - \Phi + \Phi^{3/2}\right] + \frac{\epsilon_L}{A_L}\nabla_\perp^2\Phi = 0,$$

$$A_L = a - \epsilon_L,$$

For ESW scaling: $\epsilon_L/A_L << 1$

$$\epsilon_L = (m_e/m_i)[v_{T,e\parallel}^2/(v_{z,0} - u_z)^2]$$

- 1-D parallel slab electron hole for $\partial/\partial x = \partial/\partial y = 0$

$$\Phi_{sl} = \frac{25}{16}\operatorname{sech}^4\left(\frac{z}{4}\right),$$

- Spheroidal electron hole for
  $\nabla_\perp^2 + \partial^2/\partial z^2 = \partial^2/\partial\rho^2 + (2/\rho)\,\partial/\partial\rho,$     $\rho = (x^2+y^2+z^2)^{1/2}$

- Characteristic time of parallel holes approaches $1/\omega_{p,e}$

# Oblique solution, $\partial/\partial z = \tan \theta \, \partial/\partial y$, $\tan \theta << 1$

- With the appropriate normalization we have

$$\frac{\partial^2}{\partial y^2}\left[\left(\frac{\partial^2}{\partial x^2} + \frac{\partial^2}{\partial y^2}\right)\Phi - \Phi + \Phi^{\frac{3}{2}}\right] + \eta\,\frac{\partial^2\Phi}{\partial x^2} = 0,$$

$$\eta : (m_e/m_i)\,(v_{T,e\parallel}^2/u_z^2)[(1 + \omega_{p,e}^2/\Omega_e^2)^{-1} + \tan^{-2}\theta]\; A_{LH}^{-1}.$$

$$A_{LH} = a - (m_e/m_i)(v_{T,e\parallel}^2/u_z^2)(1 + \tan^{-2}\theta).$$

- For the lower-hybrid scaling: $\eta << 1$

# Oblique solution (continued)

- 1-D oblique slab electron hole for $\partial/\partial x \to 0$

$$\Phi_{sl} = \frac{25}{16} \operatorname{sech}^4 \left(\frac{y}{4}\right),$$

- Oblique cylindrical electron hole for $\eta \to 0$
  $\partial^2/\partial x^2 + \partial^2/\partial y^2 = \partial^2/\partial r^2 + (1/r) \partial/\partial r, \ r = (x^2+y^2)^{1/2}$

$$\Phi_{cyl} \approx 2.5288 \left(1 + 0.005516 \, r^2\right)^{-0.65} I_0^{-1.6} \left(\frac{r}{1.6}\right),$$
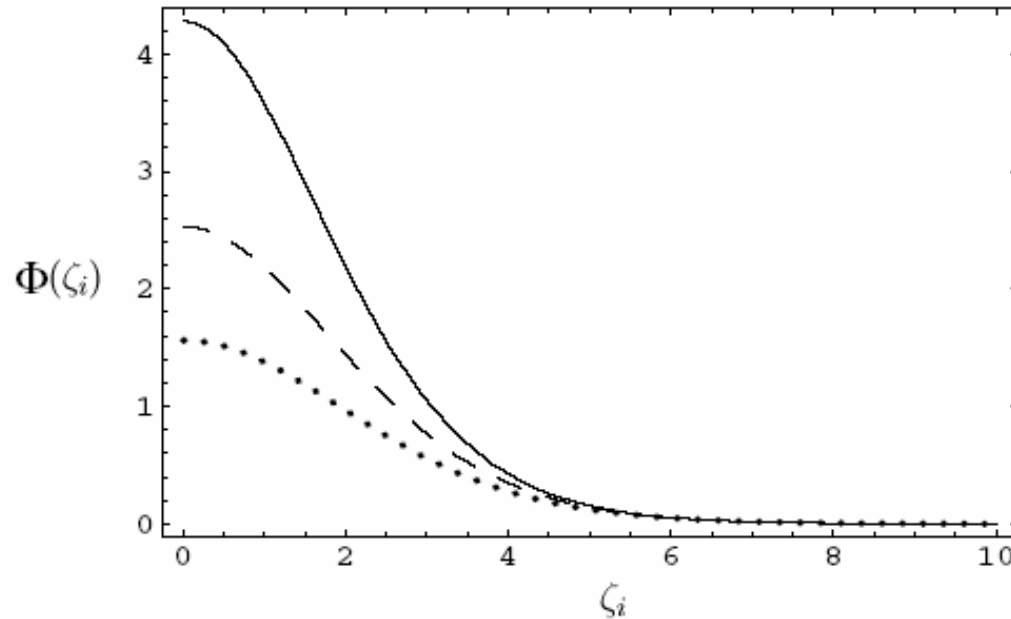
*Figure 3.* The spatial profiles of the electrostatic potentials of the magnetized electron holes. The solid, dashed, and dotted lines correspond to the spherical, cylindrical, and slab structures, respectively. The corresponding dimensionless distances
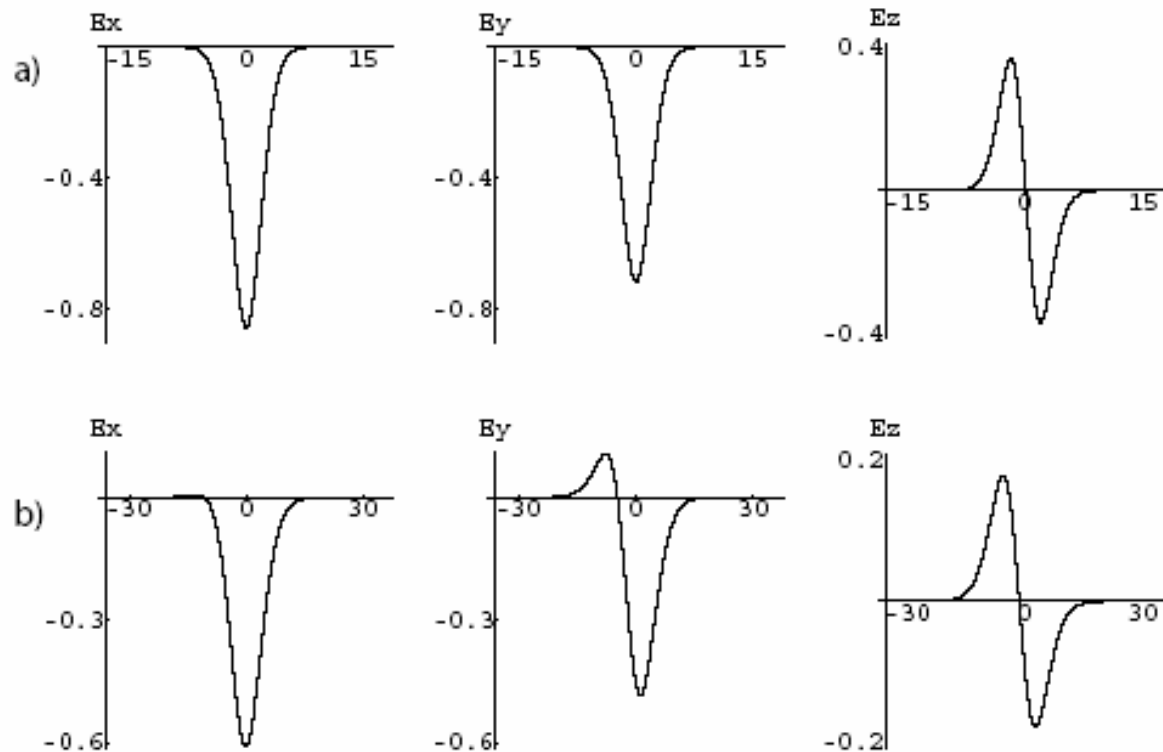
D. Jovanović, P. K. Shukla, J. Geophys. Res. **107,**

SMP 15-1 (2002)

$$\zeta_{slab} = \frac{1}{a^{1/2}} \left( \frac{x^2 + y^2}{\lambda_{D,e\parallel}^2 + \rho_{L,e\parallel}^2} + \frac{z^2}{\lambda_{D,e\parallel}^2} \right)^{1/2}, \tag{20}$$

$$\zeta_{cylinder} = \frac{y}{a^{1/2}} \left[ (1 + \tan^2\theta)\lambda_{D,e\parallel}^2 + \rho_{L,e\parallel}^2 \right]^{-1/2}, \tag{21}$$

$$\zeta_{sphere} = \frac{1}{a^{1/2}} \left[ \frac{x^2}{\lambda_{D,e\parallel}^2 + \rho_{L,e\parallel}^2} + \frac{y^2}{(1 + \tan^2\theta)\lambda_{D,e\parallel}^2 + \rho_{L,e\parallel}^2} \right]^{1/2}. \tag{22}$$

# Signals of spherical and oblique cylindrical holes



D. Jovanović, P. K. Shukla
J. Geophys. Res. **107,**

SMP 15-1 (2002)

*Figure 4.* Time dependence of the electric field components $E_x$, $E_y$ and $E_z$ corresponding to a) spheroidal and b) cylindrical ESW. In both cases $\omega_{p,e}/\Omega_e = 0.5$. Spheroidal hole is observed by a satellite located at $x = 3$, $y = 1.5$. Oblique cylindrical hole is tilted $\tan\theta = 0.6$ relative to the magnetic field, and it is observed by a satellite located at $x = 2.5$, $y = 1$. The angle between the $x$ axes and the projection of the magnetic field to the $x, y$ plane is adopted as $\varphi = 30^\circ$. The time is defined at $t = z/u_z$, and all normalizations are explained in the text.
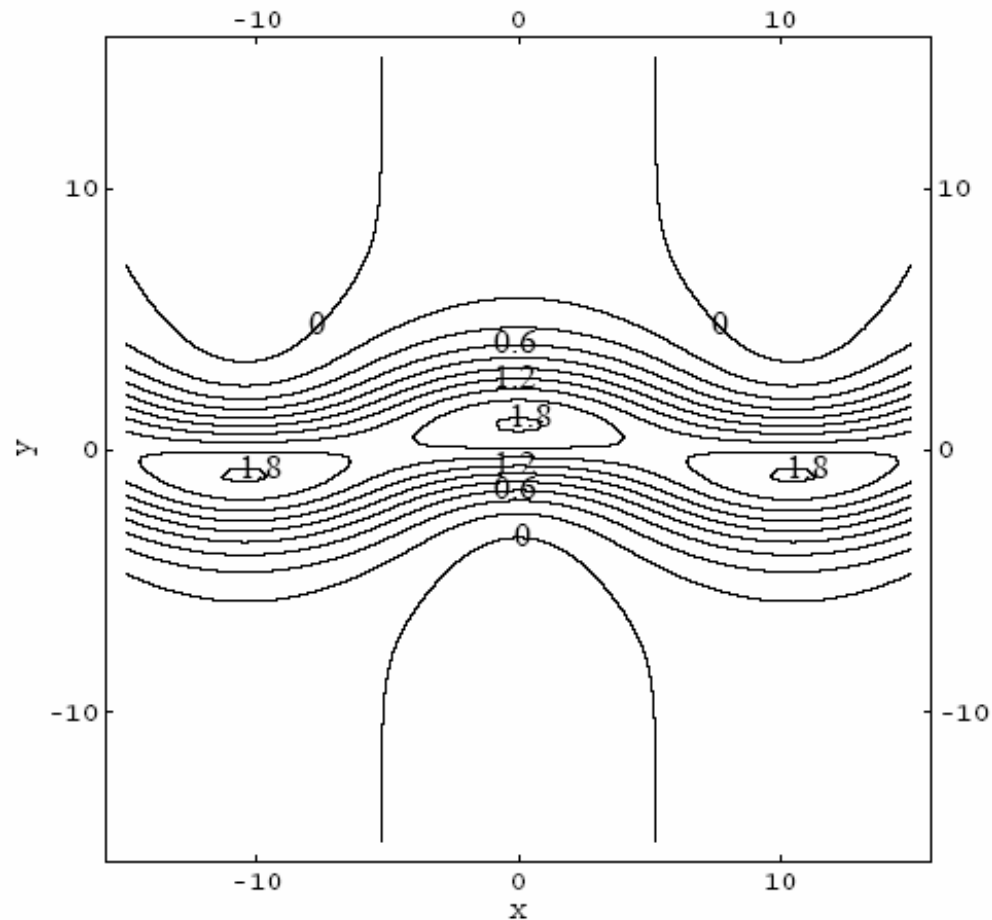
## Perpendicular instability of oblique slab holes

D. Jovanović and P. K. Shukla, (2005)

*Figure 5.* Contour plot of perturbed oblique slab lower-hybrid electron hole $\Phi(x, y) = \Phi_{sl}(y) + \delta\Phi(y) \sin(k_x x)$, with the parameters $k_x = 0.2$ and $\eta = 0.1$.

- Weakly x-dependent slab-like solution features a kink.
- In the case of an instability (e. g. due to resonance between ions and trapped electrons) the slab would fall apart (to cylinders?).

# Coupling between upper-hybrid waves and electron holes in Earth's magnetotail

- In the reconnection region there is an electron flow, which gives rise to a Buneman instability.

- In the magnetotail, the growthrate of the parallel Buneman instability (Langmuir waves) is bigger than that for lower-hybrid waves.

- The upper-hybrid waves are not excited by such beam. Their parallel phase velocity is much bigger than thermal speed and the beam is too slow.

- Both upper- and lower-hybrid waves may be excited in a four-wave coupling between stable and linearly unstable waves, which gives rise to an explosive instability (F. Verheest, J. Phys. A **15**, 1041 1982).

- Thus, the nonlinear growthrate exceeds that of the Langmuir waves!

# Coupling between upper-hybrid waves and electron holes in Earth's magnetotail (continued)

■ Separating the high- and low- frequency parts of the drift-kinetic equation, we obtain a slow equation in which the slow and ponderomotive potentials exactly add:

$$\phi_p = -\frac{e}{4m_e\omega_{\rm uh}^2}|\nabla\phi_{r,0}|^2.$$

■ Electron density is given by the same expression as for the free lower-hybrid holes, but with the total potential:

$$n_{e,s} = n_0[1 - \rho_{L,e\parallel}^2\nabla_\perp^2\Phi_{\rm tot} + a\Phi_{\rm tot} - (4/3)b\Phi_{\rm tot}^{3/2}], \qquad \Phi_{\rm tot} = e\phi_{\rm tot}/T_{e\parallel}$$

■ Slow ion response is unaffected by the ponderomotive potential:

$$\frac{\partial^2 n_{i,s}}{\partial t^2} = \frac{en_0}{m_i}\nabla^2\phi_s.$$

# Coupling between upper-hybrid waves and electron holes in Earth's magnetotail (continued)

- Low frequency Poisson's equation:

$$\frac{\partial^2}{\partial z^2}\left(\rho_{L,e\parallel}^2\nabla_\perp^2\Phi_{tot} - a\Phi_{tot} + \frac{4}{3}b\Phi_{tot}^{3/2}\right) + \left(\frac{\omega_{p,i}^2}{u_z^2} + \frac{\partial^2}{\partial z^2}\right)\lambda_{D,e\parallel}^2\nabla^2(\Phi_{tot} - \Phi_p) = 0,$$

- Standard equation for the amplitude of the upper-hybrid wave in the presence of small density perturbatons:

$$\nabla_\perp \cdot \left\{\left[2i\frac{\omega_{uh}}{\omega_{p,e}^2}\left(\frac{\partial}{\partial t} + v_{z0}\frac{\partial}{\partial z} + V_{e,s}\cdot\nabla_\perp\right) - \frac{n_{e,s} - n}{n_0} + 3\frac{T_{e\perp}}{T_{e\parallel}}\lambda_{D,e\parallel}^2\nabla_\perp^2\right]\nabla_\perp\phi_{r,0}\right\} = 0,$$

- These two coupled equations are similar to the Zakharov's system, but with a new nonlinearity due to the electron trapping in the combined slow and ponderomotive potentials

# Coupling between upper-hybrid waves and electron holes in Earth's magnetotail (continued)

- Dimensionless form:

$$\nabla_{\perp}\left[\left(i\frac{\partial}{\partial t} - \delta n_e + \nabla_{\perp}^2\right)\nabla_{\perp}\phi_{r,0}\right] = 0,$$

$$\frac{\partial^2 \delta n_e}{\partial y^2} = \alpha^2 \nabla_{\perp}^2\left(1 + \gamma^2\frac{\partial^2}{\partial y^2}\right)\left(\Phi_{tot} + |\nabla_{\perp}\phi_{r,0}|^2\right),$$

$$\frac{\partial^2}{\partial y^2}(\nabla_{\perp}^2\Phi_{tot} - \Phi_{tot} + \Phi_{tot}^{3/2}) + \frac{\varepsilon_{lh}}{A_{lh}}\frac{\partial^2\Phi_{tot}}{\partial x^2} = -\frac{\varepsilon_{lh}}{A_{lh}}\left(1 + \gamma^2\frac{\partial^2}{\partial y^2}\right)\nabla_{\perp}^2|\nabla_{\perp}\phi_{r,0}|^2,$$

$$= 0$$

- For the Cluster magnetotail data, the right-hand-side is small !!!

# Coupling between upper-hybrid waves and electron holes in Earth's magnetotail (continued)

- $\Phi_{tot}$ is readily solved as the usual electron hole:

$$\Phi_{tot}^{slab} = \frac{25}{16}\,\mathrm{sech}^4\!\left(\frac{y}{4}\right).$$

$$\Phi_{tot}^{cyl} \approx 2.53(1 + 0.005\,52\,r^2)^{-0.65}\,I_0^{-1.6}\!\left(\frac{r}{1.6}\right),$$

- Equation for the UH envelope reduces to a Gross-Pitaevskii eq., with the electron hole potential $\Phi_{tot}$ playing the role of the external potential
- The upper-hybrid waves produce a de-focussing, nonlocal nonlinearity
- Recall, the nonlocality in the envelope equation comes from the ion dynamics and the non-quasineutrality on the loer-hybrid scale
- In the 1-d slab case, the Gross-Pitaevskii equation takes the form:

$$\left[i\frac{\partial}{\partial t} + \frac{\partial^2}{\partial y^2} + \alpha^2\left(1 + \gamma^2\frac{\partial^2}{\partial y^2}\right)\left(\Phi_{tot}^{slab} + \left|\frac{\partial\phi_{r,0}}{\partial y}\right|^2\right)\right]\frac{\partial\phi_{r,0}}{\partial y} = 0.$$

# Coupling between upper-hybrid waves and electron holes in Earth's magnetotail (contd.)
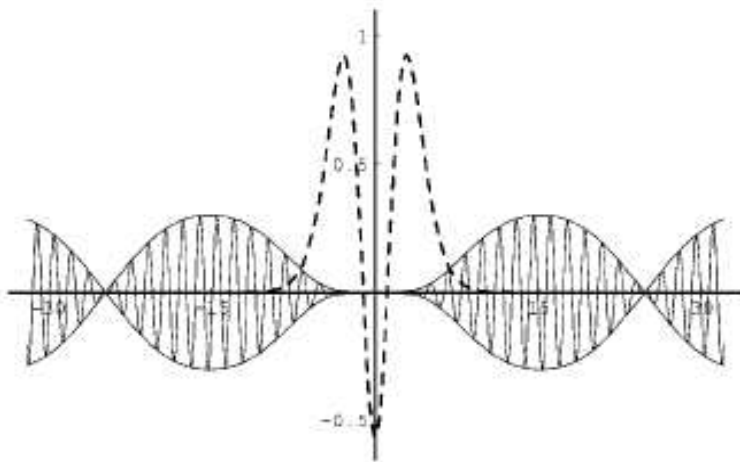


FIG. 1. Nonlinear standing wave structure. The dimensionless upper-hybrid electric field, its envelope $E$ (solid line), and the driving term $F(y) = \alpha^2(1 + \nu^2 d^2/dy^2)\Phi^{slab}_-$ (dashed line). The parameters of the solution are adopted as

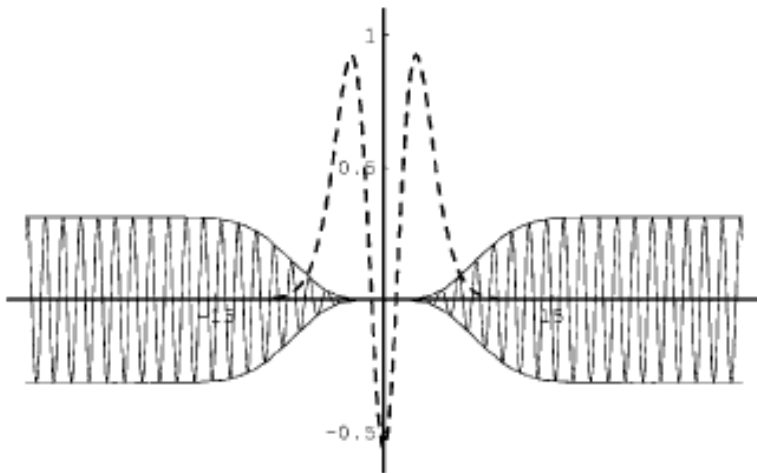- D. Jovanović and P. K. Shukla, (2005)



FIG. 2. Driven dark soliton. The notations and parameters are the same as in Fig. 1, but the boundary value $dE/dy$ at $y=0$ is slightly smaller.
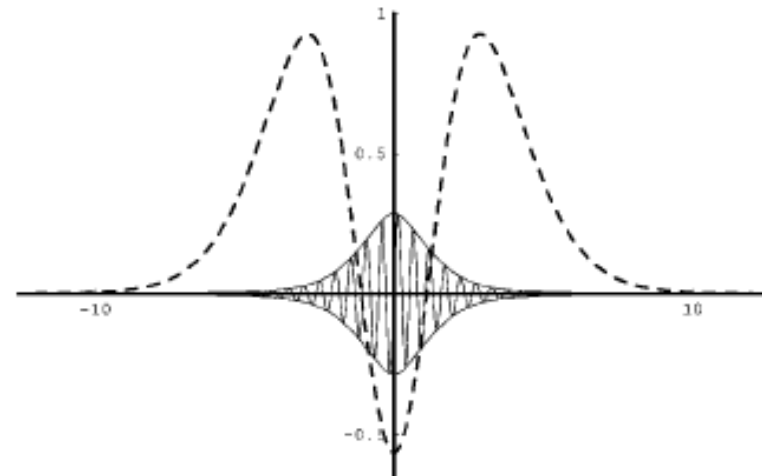


FIG. 3. Trapped bright soliton. The sign of the linear term in Eq. (21) is adopted to be $s=-1$. All other notations and parameters are the same as in Fig. 1.

# Screened double layers (tripolar ESWs)

- Allow for different levels of potential at $x = \pm\infty$
- Boltzmann distributed particles outside
- Electrons and ions trapped in adjacent potential maxima and minima

$$f_j(x, v) = \begin{cases} f_j^{(\text{free})}(v^{(0)}), & (v^{(0)} - u)^2 \geqslant -\dfrac{2q_j}{m_j}(\phi - \psi_j), \\[4mm] f_j^{(\text{trap})}(v^{(0)}), & (v^{(0)} - u)^2 < -\dfrac{2q_j}{m_j}(\phi - \psi_j), \end{cases}$$

# Screened double layers (tripolar ESWs)

- The structure consists of ½ of an electron hole, ½ of an ion hole, and ½ wavelength of a periodic nonlinear wave that traps electrons and ions in its maxima and minima.
- Such screened double layers do not require any special asymptotic boundary conditions
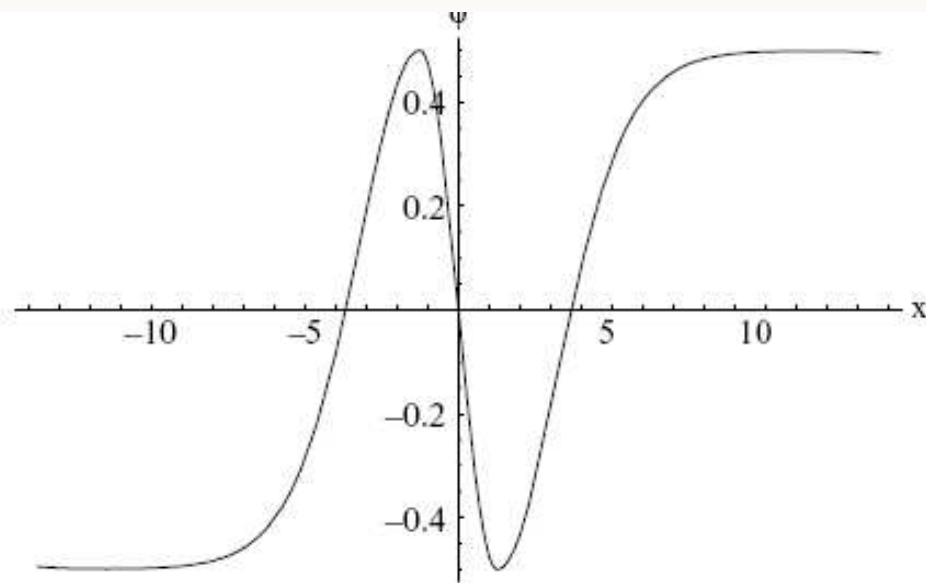
D. Jovanovic *et al.*,
J. Plasma Phys. 2005

**Figure 1.** Electrostatic potential of a small amplitude tripole. Potential is normalized to $(8/15)(b/a)(T/e)$ and the length to $4\lambda_{D,e}/\sqrt{2a}$.

# Conclusions

- We developed a drift-kinetic theory for electron phase-space vortices in magnetized plasmas in the frequency range of lower-hybrid waves.
- Our model accounts for the the ion mobility, electron polarization, anisotropic temperature and trapping in the parallel direction.
- In the small amplitude limit ⇨ Buneman instability of parallel (Langmuir) and obliquely propagating (lower hybrid) waves.
- Quasi-3-D electron holes are found, in the form of either elongated cylinders oblique to the magnetic field, or spheroids.
- Under realistic magnetospheric conditions, both hole topologies would produce similar electric field signals at the spacecraft, but for oblique cylinders a slightly larger fraction of events with bipolar pulses in the perpendicular field are expected.
- Main features of an oblique cylindrical hole (their duration, intensity and three-dimensional shape) fully coincide with those observed by the Polar mission in the magnetopause (Mozer et al., 2004).
- Standard theory of Langmuir (parallel) electron holes can not explain such very weak parallel electric fields and their long duration.

# Conclusions (continued)

- The envisaged scenario of creation of cylindrical structures starts with the oblique Buneman instability which produces a lower hybrid wave propagating almost perpendicularly to the magnetic field, whose parallel phase velocity is in the electron thermal range.

- Eventually, the linear instability saturates by the trapping of resonant electrons in the direction parallel to the guide magnetic field.

- Initially, the electron hole is predominantly one-dimensional in the form of an oblique slab.

- In the later phase the ion dynamics perpendicular to the direction of the wave propagation produces the kink (or bending) of the slab, which eventually breaks up into a "gas" of weakly interacting elongated cylindrical structures immersed in the bath of long-wavelength lower-hybrid oscillations constituting the tail of the structure.

- The electron beam may simultaneously excite both the upper- and lower-hybrid waves, in a four-wave explosive instability. Instabilty saturates by electron trapping.

- Due to the de-focusing nonlinearity 0f the upper-hybrid waves, the resulting Gross-Pitaevskii equation gives a dark soliton, but also allows for a trapped bright soliton.

# Thank you for your attention!!